

General Disclaimer

One or more of the Following Statements may affect this Document

- This document has been reproduced from the best copy furnished by the organizational source. It is being released in the interest of making available as much information as possible.
- This document may contain data, which exceeds the sheet parameters. It was furnished in this condition by the organizational source and is the best copy available.
- This document may contain tone-on-tone or color graphs, charts and/or pictures, which have been reproduced in black and white.
- This document is paginated as submitted by the original source.
- Portions of this document are not fully legible due to the historical nature of some of the material. However, it is the best reproduction available from the original submission.

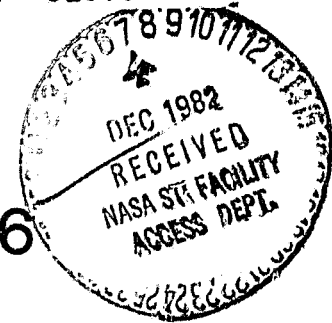
(NASA-TM-83976) THE X-RAY ABSORPTION
SPECTRUM OF 4U1700-37 AND ITS IMPLICATIONS
FOR THE STELLAR WIND OF THE COMPANION
HD153919 (NASA) 32 p HC A03/MF A01 CSCL 03B

N83-14034

G3/90 Unclas
02070



Technical Memorandum 83976



The X-Ray Absorption Spectrum of 4U1700-37 and its Implications for the Stellar Wind of the Companion HD153919

N. E. White, T. R. Kallman and J. H. Swank

AUGUST 1982

National Aeronautics and
Space Administration

Goddard Space Flight Center
Greenbelt, Maryland 20771

THE X-RAY ABSORPTION SPECTRUM OF 4U1700-37 AND ITS IMPLICATIONS
FOR THE STELLAR WIND OF THE COMPANION HD153919

N.E. White¹

Laboratory for High Energy Astrophysics
NASA/Goddard Space Flight Center
Greenbelt, Maryland 20771

T.R. Kallman²

Center for Space Research and Dept. of Physics
Massachusetts Institute of Technology
Cambridge, Massachusetts 02139

J.H. Swank

Laboratory for High Energy Astrophysics
NASA/Goddard Space Flight Center
Greenbelt, Maryland 20771

¹Also Dept. of Physics & Astronomy, Univ. of Maryland

²Supported in part by NASA Contract NAS8-30752

ABSTRACT

We present the first high resolution non-dispersive 2-60 keV X-ray spectra of 4U1700-37. The continuum is typical of that found from X-ray pulsars; that is a flat power law between 2 and 10 keV and, beyond 10 keV, an exponential decay of characteristic energy varying between 10 and 20 keV. No X-ray pulsations were detected between 160 ms and 6 min with an amplitude greater than $\sim 2\%$. The absorption measured at binary phases ~ 0.18 and ~ 0.72 is comparable to that expected from the stellar wind of the primary. The gravitational capture of material in the wind is found to be more than enough to power the X-ray source. The increase in the average absorption after $\phi \sim 0.5$, first reported by Mason et al. (1976), is confirmed. The minimum level of absorption is a factor of 2 or 3 lower than that reported by previous observers, which may be related to a factor of ~ 10 decline in the average X-ray luminosity over the same interval. Short term $\sim 50\%$ variations in absorption are seen for the first time which appear to be loosely correlated with ~ 10 min flickering activity in the X-ray flux. These most likely originate from inhomogeneities in the stellar wind of the primary. Such inhomogeneities can account for the X-ray absorption dips seen from the related supergiant systems Cyg X-1 and SMC X-1.

Subject headings: pulsar - Stars:
eclipsing binaries -
stars: individual (HD 153919) -
stars: winds - X-rays:
binaries

I. INTRODUCTION

The 3.4 day eclipsing X-ray binary system 4U1700-37/HD153919, discovered by Jones et al. (1973), distinguishes itself among the massive X-ray binaries by having the earliest spectral type primary (Hutchings 1976 and refs. therein). The strong stellar wind of HD153919 together with the moderate $\sim 10^{36}$ erg s^{-1} X-ray luminosity of 4U1700-37 suggest that the X-ray source may be driven solely by the gravitational capture of material in the stellar wind by the compact secondary (Pettersen 1978; Conti 1978). As might be expected from an X-ray emitter that is embedded in a stellar wind, the X-ray continuum is attenuated below a few keV by photoelectric absorption (Jones et al. 1973). There is an additional absorbing component evident at orbital phases greater than 0.5 (Mason, Branduardi and Sanford 1975) and the eclipse duration appears to be variable (Branduardi, Mason and Sanford 1978). The density in the stellar wind of the primary is such that the optical emission lines are formed in a region larger than the binary separation. Observed asymmetries in the radial velocities of these lines with respect to orbital phase also point to asymmetries in the stellar wind (Hammerschlag-Hensberge et al. 1973; Hutchings 1974; Hammerschlag-Hensberge 1978). X-ray flares and flickering are commonly seen on timescales of tens of minutes (Jones et al. 1973; Mason et al. 1976) with, until now, no detectable spectral change (Mason et al. 1976; Pietsch et al. 1980). The derived mass for the secondary of $\sim 1.3 M_{\odot}$ (Hutchings 1974) suggests that it is a neutron star, although coherent X-ray pulsations have not been conclusively identified (Jones et al. 1973; Branduardi et al. 1979).

We present the results of observations of 4U1700-37 by the HEAO-1 A2 experiment and the Einstein Solid State Spectrometer (SSS), Monitor Proportional Counter (MPC) and Imaging Proportional Counter (IPC). In §II

high quality non-dispersive X-ray spectra of 4U1700-37 below 20 keV are presented. We compare our results with those of past observers in §III. In the final sections we discuss the consequences of these observations for our current understanding of the mass loss process from HD153919, and for OB stars in general.

II. RESULTS

A. HEAO-1 and Einstein IPC

The ephemeris of Branduardi et al. (1978) predicts that two HEAO-1 A2[†]

[†]The A2 experiment on HEAO-1 is a collaborative effort led by E. Boldt of GSFC and G. Garmire of CIT, with collaborators at GSFC, CIT, JPL and UCB.

observations of 4U1700-37, each lasting 3 hrs, were centered at $\phi \sim 0.14$ and $\phi \sim 0.73$ on 1978 March 21 and March 23. During the former an eclipse exit occurred during earth occultation of the satellite that yields an eclipse half angle between 46° and 50° , consistent with the values seen previously (Branduardi et al. 1978). During the eclipse a residual count rate of ~ 0.018 cts $\text{cm}^{-2} \text{s}^{-1}$ was recorded by the HED (2-60 keV) corresponding to $\sim 7\mu \text{Jy}$ ($1\mu \text{Jy} \sim 1 \text{ Uhuru ct s}^{-1}$; Bradt, Doxsey and Jernigan 1979). This is similar to that seen ten days earlier when 4U1700-37 was in the scan plane of the same detector. These scanning observations reveal a previously unreported $\sim 2\mu \text{Jy}$ source somewhere on a $\sim 3^\circ$ scan line that is $\sim 1^\circ$ to the west of 4U1700-37. In order to exclude Sco X-2 from the FWHM $1.5^\circ \times 3^\circ$ FOV of the detectors the pointing direction of the satellite was offset 0.5° to the west, which brought the uncatalogued source well into the FOV. The spectrum during eclipse is significantly softer than after eclipse exit, contrary to what might be expected if the flux seen during eclipse were due to X-rays

Compton scattered around the primary by the wind, since such scattered X-rays would be greatly hardened by the effects of photoelectric absorption. We attribute this to contamination from the uncatalogued source. The contribution of this source is estimated to be at most $\sim 30\%$ of the eclipsed flux. An Einstein IPC observation was made during an eclipse on 1979 May 5 and gave only 0.04 ct s^{-1} from 4U1700-37 ($\sim 0.1 \mu\text{Jy}$ in the 0.1-4.0 keV band). This is well below the uncontaminated flux seen by HEAO-1 A2 at higher energies unless there is substantial ($\sim 10^{23} \text{ H cm}^{-2}$) low energy attenuation of the eclipsed flux. The IPC spectrum is very hard, which is in qualitative agreement with this statement. There is another significant detection in the IPC field at RA = 255.135 and Dec -37.78 with $\sim 0.06 \text{ ct s}^{-1}$ which is coincident with a ~ 9 th magnitude star. The IPC spectrum of this source is considerably softer than that of 4U1700-37, again consistent with the latter being absorbed; this new Einstein source is not related to that seen by HEAO-1 A2.

The spectra obtained from the two HEAO-1 A2 observations are summarized in Table 1. The first observation was divided into the eclipse and post-eclipse spectra. Because of the presence of the uncatalogued source in the FOV, the low energy absorption is poorly defined in all cases, in particular during eclipse. All three spectra from 4U 1700-37 can be well represented by the standard X-ray pulsar spectrum of a flat power law that is attenuated above a high energy break energy E_c by a function of the form $\exp [-(E_c-E)/E_f]$ (cf. White, Swank and Holt 1983). In all the HEAO-1 A2 observations of this source, a strong iron line between 6.4 and 6.7 keV with an equivalent width of $\sim 650 \text{ eV}$ is also required to give an acceptable fit. The break energy shows no significant variation from an average of 10 keV for all three observations. The high energy turnover of $\sim 20 \text{ keV}$ at $\phi \sim 0.72$ is

about a factor of 2 smaller after and during eclipse; the incident spectrum from the $\phi \sim 0.72$ observation is shown in Figure 1.

The data were searched for pulsations and none were found between 160 ms and 6 mins with an amplitude greater than 2 percent. For periods greater than 6 min there is considerable low frequency noise caused by ~ 10 min flickering. There was no evidence for any excess power over this noise, in particular at the previously reported but unconfirmed periods of 97 mins and 24 mins (see Branduardi et al. 1979 for a full discussion). Given the short time span of the observation and the range of variability seen, it is not meaningful to give quantitative upper limits on the amplitude of modulation at these periods.

B. Einstein SSS and MPC

4U1700-37 was observed by the Einstein SSS and MPC on 1979 March 20 and 25 at orbital phases ~ 0.73 and ~ 0.18 respectively. The MPC rate data from both observations are shown in Figure 2 with a time resolution of 50s. Also shown is the hardness ratio of the flux in the 5-10 keV band over that in the 2-5 keV bands (hardness ratio). The ubiquitous ~ 10 min flickering and flaring can be clearly seen, together with a factor of 3 flare at ~ 13 hrs on March 25. The average hardness ratio is larger at later orbital phases. In addition there are previously unobserved fluctuations in the hardness ratio on timescales similar to the flickering. There is a tendency for the hardness ratio to be a minimum at times of minimum flux, although the correlation is loose. For example at 14-15 hrs on Day 79 the hardness ratio tracked one flare but then during the next flare did not. Figure 3 shows the hardness ratio versus count rate for each of the observations. The hardness ratio and count rate during these two observations have linear correlation coefficients of 0.48 and 0.63, respectively and the probability that these values for the

correlation coefficient would be found for two statistically uncorrelated samples are < 0.001 (Bevington 1978). A cross correlation shows no evidence for a time delay between the hardness and intensity, for time delays more than ~ 100 sec.

We summed the SSS spectral data into three groups corresponding to the non-flare and flare data near $\phi \sim 0.18$ and all the data from $\phi \sim 0.73$. The spectral parameters obtained from the SSS data are summarized in Table 2. The power law energy index α was fixed at the HEAO-1 A2 value of -0.15 , although the results are insensitive to variations in this parameter within the uncertainties quoted in Table 1. There is an increase in the absorption from $(1.0 \pm 0.2) \times 10^{23} \text{ H cm}^{-2}$ to $(1.6 \pm 0.2) \times 10^{23} \text{ H cm}^{-2}$ (90% confidence) between the two binary phases. This change is accompanied by an overall increase in the MPC hardness ratio between $\phi \sim 0.18$ and $\phi \sim 0.73$ (Figure 2), leading us to attribute the hardness ratio changes to changing absorption, rather than to changes in the continuum. This view is further supported by the lack of any variation in the high energy continuum on similar timescales (Pietsch et al. 1980). There is no significant change in absorption associated with the flare at $\phi \sim 0.19$ relative to the average of all the remaining data in that interval. In Figure 4 the $\phi \sim 0.18$ flare plus the non-flare PHA data and all the $\phi \sim 0.73$ PHA data are shown along with the best fit model. Attempts to resolve spectral changes with the SSS on shorter timescales were unsuccessful due to the low count rate. The magnitude of the short timescale variations in the MPC hardness ratio are comparable with the average change from $\phi = 0.18$ to 0.73 and indicates that we are observing 50% fluctuations in absorption.

III. COMPARISON WITH PAST OBSERVATIONS

The increase in absorption we observed at later orbital phases (cf.

Figure 2, Table 2) is similar to that reported by Mason et al. (1976) and Branduardi et al. (1978) from Copernicus observations; although the minimum value of the low energy absorption seen by the SSS was a factor 2-3 lower. Such a difference cannot be caused by systematic differences in the dynamic range and resolution of the two experiments. The MPC is to lowest order a much larger version of the Copernicus 2-10 keV detector and would be similarly affected; the column densities implied by the MPC, while less precise, are not systematically higher than the SSS values.

The factor of 2-3 long term decrease in absorption may be related to a factor of 10 reduction in the average X-ray luminosity of the source. In Table 3 we summarize the range of absorption and of flux seen by ourselves and past observers. The latter is given in units of μJy for those intervals where the absorption was less than $4 \times 10^{23} \text{ H cm}^{-2}$. Given the difference between the various detectors these may be uncertain by up to $\sim 50\%$. Table 3 illustrates a rough correlation between the minimum value of the absorption and the average intensity of the source. The luminosities seen by Dolan et al. (1980) and Pietsch et al. (1980) in 1978 Sept. and Nov. are comparable with those given in Tables 1 and 2. These results provide convincing evidence of a systematic decrease in intensity and absorption since 1974.

Mason et al. (1976) reported that there is no spectral variability associated with the flaring activity. Our discovery of $\sim 50\%$ changes in absorption associated with the variability is probably not in contradiction with this earlier result because the limited sensitivity of the Copernicus detector forced Mason et al. (1976) to apply a simple intensity filter over several days of data. As is well illustrated by Figure 3 this would tend to include both high and low absorption data.

Measurements of the continuum above $\sim 20 \text{ keV}$ by high energy experiments

gives an exponential attenuation energy E_F of ~ 30 keV (Dolan et al. 1980; Pietsch et al. 1980), although Ricker et al. (1970) finds a lower E_F of 10-20 keV. Our observations show evidence for a variation in E_F from 10 to 20 keV at different orbital phases. Some of these differences may reflect the different dynamic ranges of the various experiments, however our data also suggests some intrinsic variation. The average flux after eclipse exit is a factor of two below that seen at $\phi \sim 0.72$ (Table 1). This lower intensity may be coincidental, although past observations on occasion also show evidence for a gradual eclipse entry/exit (Branduardi et al. 1978). Since there is no substantial increase in absorption associated with this reduction in flux it may suggest the presence of a substantial optical depth of hot fully ionized material close to the surface of the primary; Compton scattering in this material could also be responsible for the change in the parameter E_F .

IV. THE ACCRETION FLOW

The absorbing column that we measure can be compared with that predicted on the basis of the known parameters of the system, assuming all the absorption is from the stellar wind. We use the parameters of this system summarized by Conti (1978), together with the stellar wind velocity law $v(R) = v_\infty (1 - R_*/R)^\gamma$, where R is the distance from the center of the primary, R_* is the primary radius, v_∞ is the terminal velocity, and $\gamma = 0.5$ or $\gamma = 1$. Such a model assuming a mass loss rate of $10^{-5} M_\odot \text{ yr}^{-1}$ and $v_\infty = 2600 \text{ km s}^{-1}$ (Dupree et al. 1978) yields an estimate of the cold column density expected at orbital phase $\phi = 0.18$ of $N_{1.0} = 2.1 \times 10^{23} \text{ H cm}^{-2}$ for $\gamma = 1.0$ and $N_{0.5} = 1.4 \times 10^{23} \text{ H cm}^{-2}$ for $\gamma = 0.5$; these values are $\sim 15\%$ smaller at $\phi \sim 0.72$. The latter estimate is in reasonable agreement with the observed value of $(1.0 \pm 0.2) \times 10^{23} \text{ H cm}^{-2}$. The slight discrepancy can in part be attributed to partial ionization of the stellar wind by the X-ray source,

which reduces the effective cross section of the material along the line of sight. These estimates are also sensitive to uncertainties in the assumed primary mass loss rate.

Following the simple stellar wind accretion model outlined by Davidson and Ostriker (1973) the mass transfer rate required to produce the observed luminosities assuming 100% conversion of the gravitational potential energy into X-rays and spherical symmetry, is given by $\dot{M} \sim 10^{-6} \cdot L_{36} \cdot v_3^4 M_\odot \text{ yr}^{-1}$ where L_{36} is the observed luminosity in units of $10^{36} \text{ erg s}^{-1}$ and v_3 is the wind velocity at the X-ray source in 1000 km s^{-1} (a neutron star with a mass of $1.4 M_\odot$ is assumed). The velocity of the wind in the vicinity of the X-ray source will be equal to the wind velocity at the point where the X-ray source photoionizes the ionic species responsible for the radiative acceleration of the wind (Hatchett and McCray 1976); the material presumably coasts beyond this point. According to this criterion, the radiative acceleration will be suppressed throughout a roughly spherical volume of radius $\sim 10^{11} \text{ cm}$. The aforementioned velocity law gives velocities of $\sim 20\%$ and $\sim 44\%$ the terminal values for $\gamma = 1.0$ and 0.5 respectively. These require a mass loss rate from the primary of $< 10^{-6} M_\odot \text{ yr}^{-1}$, compared to the assumed value for this type of star of $10^{-5} M_\odot \text{ yr}^{-1}$. Alternatively a mass loss rate of $10^{-5} M_\odot \text{ yr}^{-1}$ requires a wind velocity near the X-ray source of $\sim 1900 \text{ km s}^{-1}$ in order to produce the observed X-ray luminosities; this exceeds the wind velocity predicted by the simple velocity law by a factor of ~ 4 , for a terminal velocity $v_\infty = 2600 \text{ km sec}^{-1}$ and $\gamma=1$. There is clearly no need to invoke an additional source of material from Roche lobe overflow, since we already have more than is required. This discrepancy may indicate that the velocity law is faster than expected which in turn would also help reduce the overestimate of the predicted absorption discussed earlier.

The reduction in the base level of the absorption associated with a decrease in the average intensity between these results and those of past observers supports the idea that both the accreted material fueling the X-ray source, and the material responsible for the absorption originate in the stellar wind. While there is uncertainty in the mean intensity, this correlation does not appear to be linear (Table 3) which suggests that if wind accretion dominates, then the velocity of the wind in the vicinity of the X-ray source must be changing along with any change in the mass transfer rate.

The residual flux seen during eclipse of $\sim 10\%$ the average uneclipsed emission is consistent with that expected from scattering of the original emission by the stellar wind around the primary. For the optically thin case the flux scattered around the primary will be $\sim \tau$ times the uneclipsed value, where τ is the average optical depth through the wind. The scattered flux implies $\tau \sim 0.1$ which in turn gives $\sim 10^{23} \text{ H cm}^{-2}$, consistent with both that derived above and the absorption inferred from the low count rate seen by the IPC.

Although the absorption seen at $\phi = 0.18$ can be reconciled with the other parameters of the binary system, the $\sim 50\%$ asymmetry between the absorption seen at $\phi = 0.18$ and that seen at $\phi = 0.73$ cannot be so easily understood. The simple theory of stellar wind absorption (Buff and McCray 1974) predicts that the absorption should be symmetric about $\phi = 0.5$, and that the phases closest to eclipse exhibit the strongest absorption. Phase related absorption asymmetries have also been observed in the other massive X-ray binaries Cen X-3 (Schreier et al. 1972) and Vela X-1 (Charles et al. 1978; Kallman and White 1982).

The interpretation of the gas flows in 4U1700-37 and the other systems where asymmetries have been observed is complicated by the great variety of

physical processes that may be acting. If the accretion occurs via Roche lobe overflow, Prendergast and Taam (1974) have shown that the accretion flow may tend to fill the region trailing the X-ray source in its orbit, presumably leading to asymmetric absorption similar to that observed. If the accretion occurs directly from the stellar wind (Davidson and Ostriker 1973), then the supersonic motion of the X-ray source through the wind may produce an "accretion wake" downstream from the X-ray source (Eadie et al. 1975). The material in the wake, although heated by passage through the shock wave trailing the X-ray source and by X-ray photoionization, may still be able to produce the observed absorption. Simple estimates show that the accretion wake can produce extended regions of absorption centered on roughly orbital phases 0.5 and 0.7 (Jackson 1975). However, as noted by Mason et al. (1976) and Branduardi et al. (1978), the extended region of enhanced absorption at later orbital phases argues against the accretion wake as an explanation for the asymmetric absorption from 4U1700-37. Fransson and Fabian (1980) proposed that shocks formed in the collision of radiatively driven wind with the part of the wind photoionized by the X-ray source (but still subject to the massive star's gravity) could give rise to the asymmetric density structure.

V. THE STRUCTURE OF THE STELLAR WIND OF HD153919

The $\sim 50\%$ variation in the absorption on a timescale similar to that of the X-ray flickering suggests that we are viewing optically thick blobs of material attenuating the X-ray source, and that these same inhomogeneities are responsible for the flickering via variations in the accretion rate. Although such absorbing blobs could arise from instabilities in the accretion flow near the neutron star magnetosphere, the material there is likely to be highly ionized, and the freefall timescale for such instabilities much smaller than the ~ 10 min timescale we observe (Brinkmann 1981). A more likely origin is

blob-like inhomogeneities in the stellar wind which, since the accretion flow is likely dominated by capture from the wind, provides a natural explanation for the flickering and absorption. The flickering may be caused by episodes of enhanced accretion, while the absorption events may be the blobs passing through our line of sight. The observed loose correlation between absorption and flickering then may be due to the fact that some of the blobs along the line of sight escape capture by the neutron star, while others are entirely swallowed, leading to a range of possible absorption/emission ratios.

If we assume the velocity of the wind is $\sim 10^3$ km s⁻¹ the timescale of the flickering of ~ 10 mins gives a thickness for the inhomogeneities in the direction of velocity vector of $\sim 6 \times 10^{10}$ cm. We cannot distinguish between the absorption events and X-ray flickering being caused by either factor of 2 or 3 density enhancements, or by factor of ~ 2 variations in the velocity of the wind (or perhaps by a combination of both). The 50% changes in absorption implied by the hardness ratio are equivalent to $\sim 5 \times 10^{22}$ H cm⁻² variations in the line of sight column density. Using a mass loss rate of $10^{-5} M_{\odot}$ yr⁻¹ and the velocity law with $\gamma = 0.5$ gives a density in the vicinity of the X-ray source of $\sim 10^{11}$ cm⁻³ which, in view of the overestimate of the X-ray luminosity, can be regarded as a conservative upper limit. This indicates that to give sufficient absorbing column the blobs must be elongated in our viewing direction. Further evidence for an elongated structure comes from the fact that all the low-Z elements within a radius of $\sim 10^{11}$ cm, similar to the blob thickness, will be fully ionized by the X-ray source. For the cases where there are correlated flare and absorption events this again requires more material further away in the line of sight. Because all the observations were made close to quadrature, when we view approximately perpendicular to the velocity vector of the wind in the vicinity of the X-ray source, the blobs

must be flattened in the direction of their velocity vector. The observed absorption variations give a larger dimension for the blobs of $\gtrsim 5 \times 10^{11}$ cm; further observations at different orbital phases may allow their exact size to be directly measured. We expect that observations at the superior conjunction of the X-ray source (where we have none) will reveal the absorption events to be much less pronounced.

According to this model the only blobs which will practice significant fluctuation in absorption will be those which graze the X-ray Stromgren zone. These same blobs will also produce emission via enhanced accretion. Of the blobs which emit, we expect about half to absorb also, since this fraction will pass along the observer's line of sight. This is roughly in accord with the correlation we observe.

These inhomogeneities may be the same as those proposed by Lucy and White (1980) to account for the coronal X-ray emission seen from OB stars. The anomalous ionization state of the X-ray absorbing material seen on occasions from Vela X-1 also requires a source of soft X-rays distributed throughout the wind (Kallman and White 1982). Similar timescale flickering and flaring activity has been seen from Vela X-1 (Charles et al. 1978), X Per and γ Cas (White et al. 1982); although the wind density is smaller in these systems and absorption events would probably not be detectable by current instrumentation. This supports the view that stellar wind accretion also dominates in these systems and that the structure of the wind is similar. In other related systems where gas streams may dominate the flow to the X-ray source (Conti 1978; Petterson 1978) such flickering and flaring are not seen (SMC X-1: Marshall, White and Becker 1983; Cen X-3: Schreier et al. 1972; Cyg X-1: Mason et al. 1974). Absorption events are also not usually seen from these systems because the high luminosity of the X-ray source will fully

ionize most of the stellar wind on the X-ray source side of the primary. SMC X-1 has recently been observed to undergo absorption events close to eclipse, i.e. when we view close to the primary where the ionization of the wind by the X-ray source is reduced; the timescale of these events is again comparable to those discussed here but their column density is an order of magnitude higher (Marshall et al. 1983). Similarly, inhomogeneities in the wind of the primary of Cygnus X-1 can account for the absorption dips that have been reported near superior conjunction of the primary (Mason et al. 1974; Li and Clark 1974). The peculiar nature of the absorption spectrum of these dips below ~ 4 keV found by Pravdo et al (1980) may be caused by partial ionization of the blobs. Clearly these systems are allowing new insight into the structure of the stellar wind of OB stars.

VI. THE NATURE OF THE SECONDARY

The failure to detect any X-ray pulsations from 4U1700-37 is surprising given the close resemblance of the properties of this system to other OB binary stars that have pulsating X-ray secondaries (e.g. Vela X-1; McClintock et al. 1976). The 2-60 keV spectrum that we present (Figure 1) is very similar to the phase averaged spectra of X-ray pulsars in general (White et al. 1983). This adds further circumstantial evidence that the compact object is an accreting neutron star. γ Cas and 2S0114+65 ($L_x \sim 10^{32}-10^{34}$ erg s $^{-1}$) are similar cases where probably there are accreting magnetic neutron stars that do not impose coherent periodicity on the observed flux (White et al. 1982; Koenigsberger et al. 1982). If the neutron stars in 4U1700-37, γ Cas and 2S0114+65 are undergoing spherical accretion from the stellar wind then the infalling material will enter the screening currents of the magnetosphere via the Rayleigh-Taylor instability. The material is not easily attached to the field lines and it will not form a well collimated flow to the magnetic

pole (Arons and Lea 1976a,b; Elsner and Lamb 1977). Arons and Lea (1980) have shown that when $L_x < 10^{36}$ erg s⁻¹ a substantial fraction of the infalling material may rain down all over the neutron star surface and thus make any modulation of very low amplitude and hard to detect. Several of the low luminosity stellar wind accreting neutron stars do tend to show much less structured and smaller amplitude light curves than is seen from the more luminous systems (White et al. (1983). It is therefore quite plausible that in 4U1700-37 the accretion process and viewing conditions are such that X-ray pulsations cannot be detected.

It is interesting to compare the properties of Vela X-1 with those of 4U1700-37. As is the case for 4U1700-37 (cf. § IV), there is more than enough material in the stellar wind to power the X-ray source (Conti 1978; Petterson 1978), which makes it unnecessary to invoke any major contribution from Roche lobe overflow. But the fact that strong pulsations are detected from Vela X-1 is in stark contrast to the lack of any from 4U 1700-37. This may reflect a fundamental difference in the accretion process. For example, even a small accretion disk surrounding the neutron star in Vela X-1 may allow much more efficient threading of the accreted material onto the field lines (Ghosh and Lamb 1979).

The similarity of the spectrum of 4U1700-37 to spectra of pulsars extends to the equivalent width of an emission feature attributable to Fe. The equivalent widths are about the same as for 4U1145-61 and 4U1258-52 which also have luminosities 10^{35} - 10^{36} ergs s⁻¹ (White et al. 1983). With limits of 20 days on their binary periods they are likely to be wind accretors and White et al. saw for them no alternative production site for Fe emission than matter accumulated with optical depth > 0.1 at the magnetospheres of the pulsars. In the case of 4U1700-37 the close stellar companion and denser wind do allow

(for $N_{\text{Fe}}/N_{\text{H}} \sim 4 \times 10^{-5}$) perhaps 90 eV, at most, from the star, (Basko 1978; Hatchett and Weaver 1977) and perhaps 360 eV from the wind if we consider both 6.4 keV and 6.7 keV complexes (Hatchett and McCray 1978). While the wind structure and its contribution are uncertain, it is unlikely that it and the companion can account for the full effect. The shortfall would be explained if there is also accumulation at a magnetosphere around a neutron star in 4U1700-37. (However, the approximate equality of the equivalent widths for 4U1700-37 and the pulsars would be a coincidence.)

VII. CONCLUSION

These observations support the idea that the stellar wind of HD153919 is the dominant influence on the observed X-ray properties. Conversely this means the X-ray source is providing information on the nature of the stellar wind. The dense region of material following the X-ray source in this and all other related systems cannot be reasonably accounted for in the context of current accretion wake or Roche lobe overflow models. On shorter time-scales 50% fluctuations in absorption on timescales of ~ 10 min shows that wind is inhomogeneous and contains blobs of material, flattened in the direction of their velocity vector, with a thickness of $\sim 6 \times 10^{10}$ cm and a width at least an order of magnitude larger. Similarly structured winds from the primaries of Cyg X-1 and SMC X-1 can account for the absorption dips seen from these systems. Lucy and White (1980) and Lucy (1982) have invoked the non-uniform acceleration of such inhomogeneities as the origin of shocks in the wind that are responsible for the soft X-ray coronal emission seen from all OB stars. X-ray observations of these massive X-ray binary systems at different binary phases will allow our knowledge of the structure and origin of these inhomogeneities to be further refined. This may turn out to be the only direct method of measuring the fine structure of the stellar winds of early

type stars.

ACKNOWLEDGMENTS

We thank Allyn Tennant, Frank E. Marshall and Graziella Branduardi-Raymont for helpful discussions and Steve Holt for his advice, encouragement, and sense of humor.

TABLE 1: HEAO-1 A2 RESULTS

Binary Phase ϕ	0.125-0.138b (eclipsed)	0.138-0.162	0.706-0.747
Day 1978	80	80	82
Average HED ct s ⁻¹ cm ⁻²	0.018	0.05	0.11
L_x^a (erg s ⁻¹)	1×10^{35}	2×10^{35}	7×10^{35}
Energy index α	0.1 ± 0.3	0.0 ± 0.2	-0.15 ± 0.15
N_H (H cm ⁻²)	-----	$< 14 \times 10^{22}$	$5^{+7}_{-3} \times 10^{22}$
E_C (keV)	10 ± 5	10 ± 3	10 ± 2
E_F (keV)	13 ± 5	11 ± 4	20 ± 3
Iron K α Line			
EW (eV)	800 ± 400	650 ± 120	630 ± 90
ΔE (keV)	< 3	< 3	< 3
χ^2/dof	21/30	35/30	27/30

^a the unabsorbed luminosity in the 1-100 keV band for an assumed distance of 1.2 kpc (Hutchings 1976)

^b all the spectra are contaminated by an uncatalogued soft $\sim 2 \mu\text{Jy}$ source $\sim 1^\circ$ to the west of 4U1700-37. This spectrum is particularly badly contaminated and the flux may be over estimated by up to $\sim 30\%$ and the hydrogen absorption derived is unreliable.

TABLE 2: EINSTEIN SSS

Orbital Phase ϕ	0.172-0.202	0.191	0.714-0.764
Day (1979)	84	84	79
Average SSS cts s ⁻¹	0.70	1.30	0.55
L_x^a (erg s ⁻¹)	7×10^{35}	2×10^{36}	9×10^{35}
Normalization	0.060	0.144	0.081
Energy index α (Fixed)	0.85	0.85	0.85
N_H (10^{22} H cm ⁻²)	10 ± 2	11 ± 1	16 ± 2
χ^2/dof	71/50	46/50	90/50

^a the unabsorbed luminosity in the 1-100 keV energy band for an assumed distance of 1.2 kpc (Hutchings 1976).

TABLE 3: THE HISTORY OF 4U1700-37

Date	Satellite	Average Range of Flux (μJy)	$N_{\text{H}} \times 10^{22}$ (H cm^{-2})
1974 July	Copernicus ^a	100-260	25-60
1975 July	Copernicus ^b	30-120	21-60
1976 August	Copernicus ^b	20-80	18-50
1978 March	HEAO-1 A2 ^c	10-30	< 15
1979 March	Einstein ^c	10-30	10-16

^a Mason, Branduardi and Sanford (1976)

^b Branduardi, Mason and Sanford (1978)

^c This work

REFERENCES

- Arons, J., and Lea, S.M., 1976a, *Ap. J.* 207, 914.
- Arons, J., and Lea, S.M., 1976b, *Ap. J.* 210, 792.
- Arons, J., and Lea, S.M., 1980, *Ap. J.* 235, 1016.
- Basko, M.M., 1978, *Ap. J.* 223, 268.
- Bradt, H.V., Doxsey, R.E., and Jernigan, J.G., 1979, *Adv. Space Exp* 3, 3.
- Branduardi, G., Mason, K.O., Sanford, P.W., 1978, *M.N.R.A.S.* 185, 137.
- Branduardi, G., Dupree, A.K., Sanford, P.W., and Pollard, G.S.G., 1979, *Nature* 279, 508.
- Brinkmann, W., 1981, *Astr. Ast.* 94, 323.
- Buff, J., and McCray, R., 1974, *Ap. J.* 188, 63.
- Castor, J.I., Kallman, T.R., McCray, R.A., Olson, G., 1982, in preparation.
- Charles, P.A., Mason, K.O., White, N.E., Culhane, J.L., Sanford, P.W., and Moffatt, A.J.F., 1978, *M.N.R.A.S.* 183, 813.
- Conti, P., 1978, *Astr. Ap.* 63, 225.
- Davidson, K., and Ostriker, J.P., 1973, *Ap. J.* 179, 585.
- Dolan, J.F., Coe, M.J., Crannell, C.J., Dennis, B.R., Frost, K.J., Maurer, G.S., and Orwig, L.E., 1980, *Ap. J.* 238, 28.
- Dupree, A.K., et al., 1978, *Nature* 275, 400.
- Eadie, G., Peacock, A., Pourids, K.A., Watson, M., Jackson, J.C., and Hunt, R., 1975, *M.N.R.A.S.* 172, 35p.
- Elsner, R.F., and Lamb, F.K., 1977, *Ap. J.* 215, 897.
- Fransson, C., and Fabian, A.A. 1980, *Astr. Ap.* 87, 102.
- Ghosh, P., and Lamb, F.K., 1979, *Ap. J.* 232, 259.
- Hammerschlag-Hensberge, G., van den Heuvel, E.P.J., and Paesde Banco, M.H., 1973, *Astr. Ap.* 29, 69.

- Hammerschlag-Hensberge, G., 1978, Astr. Ap. 64, 399.
- Hatchett, S., and McCray, R., 1977, Ap. J. 211, 522.
- Hatchett, S., and Weaver, R. 1977, Ap. J. 215, 285.
- Hutchings, J.B., 1974, Ap. J. 112, 677.
- Hutchings, J.B., 1976, X-Ray Binaries (NASA S-389), 531.
- Jackson, J.C., 1975, M.N.R.A.S. 172, 483.
- Jones, C., Forman, W., Taranbaum, H., Schreier, E., Gursky, H., Kellogg, E.,
and Giacconi, R., 1973, Ap. J. 181, L43.
- Kallman, T.R., and McCray, R.A., 1982, Ap. J. Supp, in press.
- Kallman, T.R., and White, N.E., 1982, Ap. J. (Letters), in press.
- Koenigsberger, G., Swank, J.H., Szymkowiak, A.E., and White, N.E., 1983, in
preparation.
- Li, F.K., and Clark, G.W., 1974, Ap. J. 191, L27.
- Lucy, L.B., and White, R.L., 1980, Ap. J. 241, 300.
- Marshall, F.E., White N.E., and Becker, R.H., 1982, Ap. J., submitted.
- Mason, K.O., Hawkins, F.J., Sanford, P.W., Murdin, P., and Savage, A., 1974,
Ap. J. 192, L65.
- Mason, K.O., Branduardi, G., and Sanford, P.W., 1976, Ap. J. 203, L29.
- McClintock, J.E. et al., 1976, Ap. J. 206, L99.
- Peterson, J.A., 1978, Ap. J. 224, 625.
- Pietsch, W., Voges, W., Reppin, C., Trumper, J., Kendziorra, E., and Staubert,
R., 1980, Ap. J. 237, 964.
- Pravdo, S.H., White, N.E., Kondo, Y., Becker, R.H., Boldt, E.A., Holt, S.S.,
Serlemitsos, P.J., and McCluskey, G.E., 1980, Ap. J. 237, L71.
- Prendergast, K.H., and Taam, R.E., 1974, Ap. J. 189, 125.
- Ricker, G.R., Gerassimenko, M., McClintock, J.E., Ryckman, S.G., and Lewin,
W.H.G, 1976, Ap. J. 207, 333.

Schreier, E., Giacconi, R., Gursky, H., Kelley, E., and Tananbaum, H., 1972,

Ap. J. 178, L71.

White, N.E., Swank, J.H., Holt, S.S., and Parmar, A.N., 1982, Ap. J., in
press.

White, N.E., Swank, J.H., and Holt, S.S., 1983, to be published in Ap. J.

FIGURE CAPTIONS

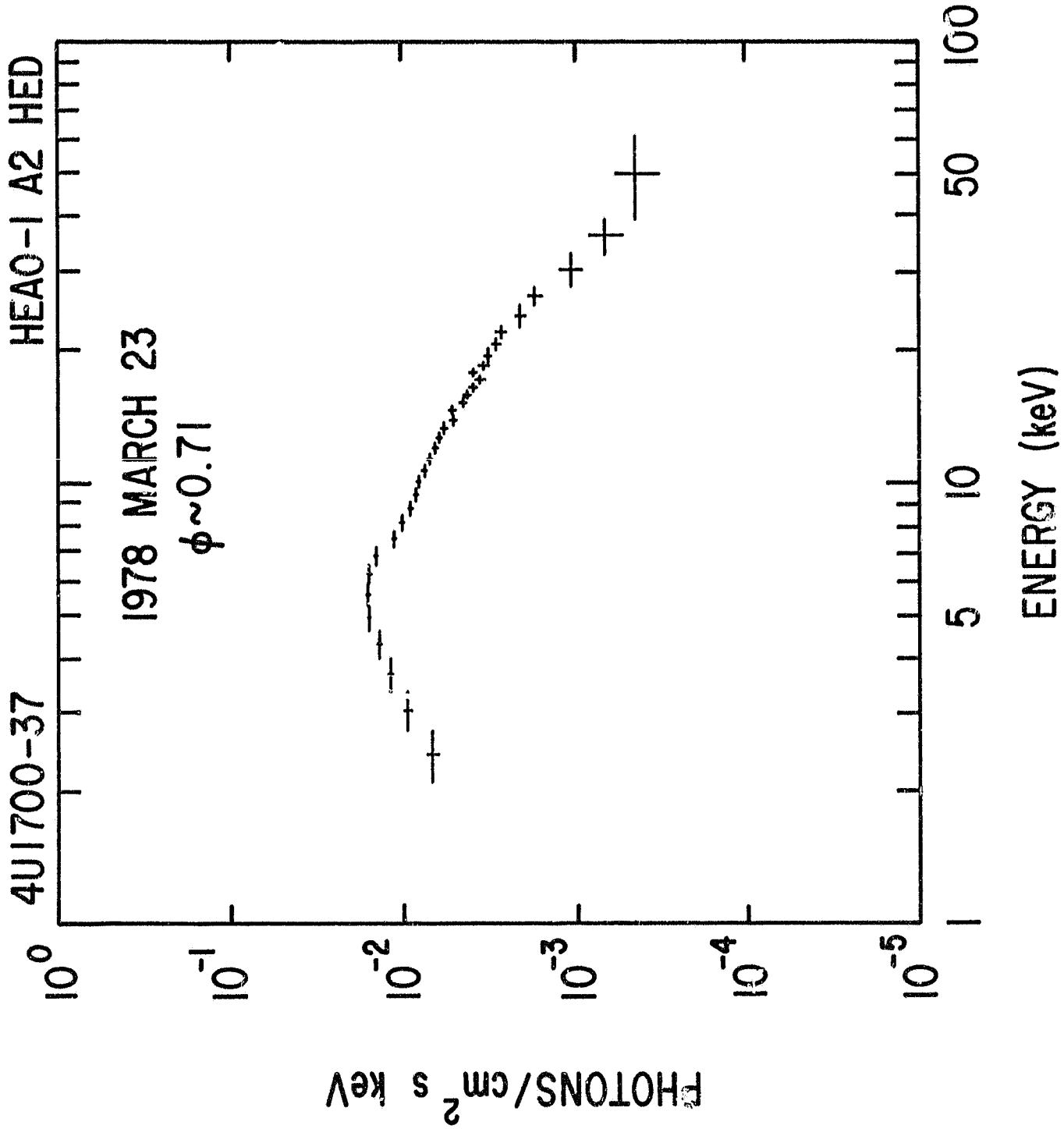
Figure 1 - The incident spectra of 4U1700-37 at $\phi \sim 0.72$ from the HED detector of HEAO-1 A2, deconvolved using the best fit model given in Table 1.

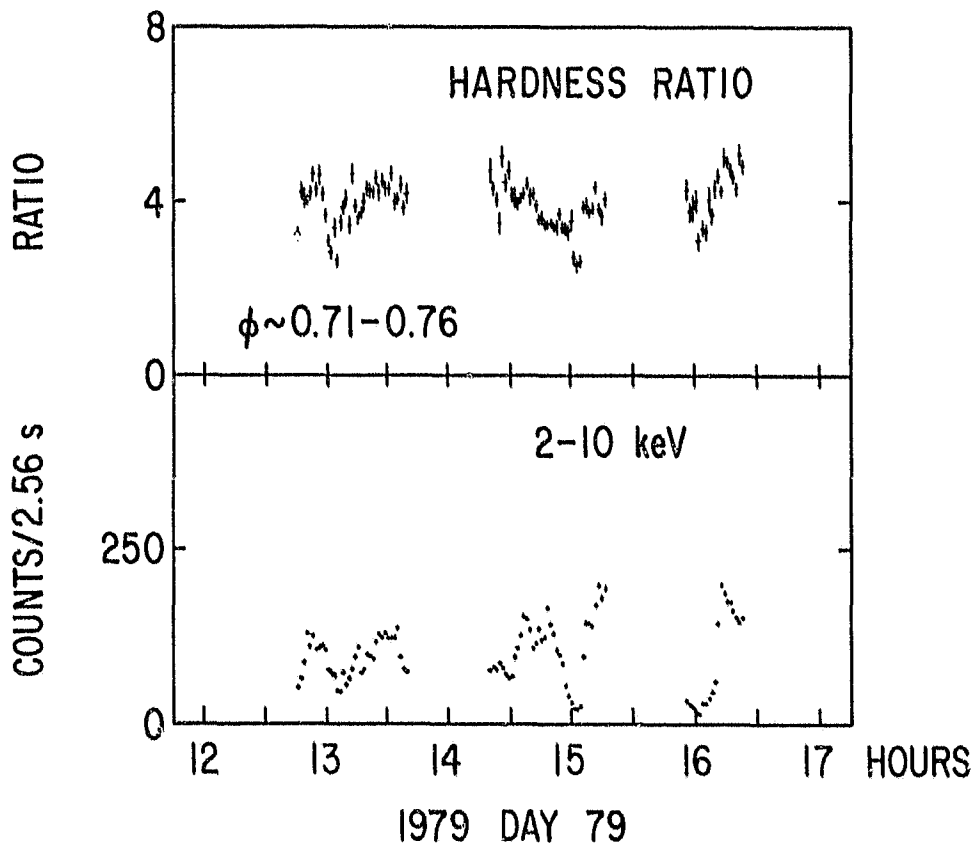
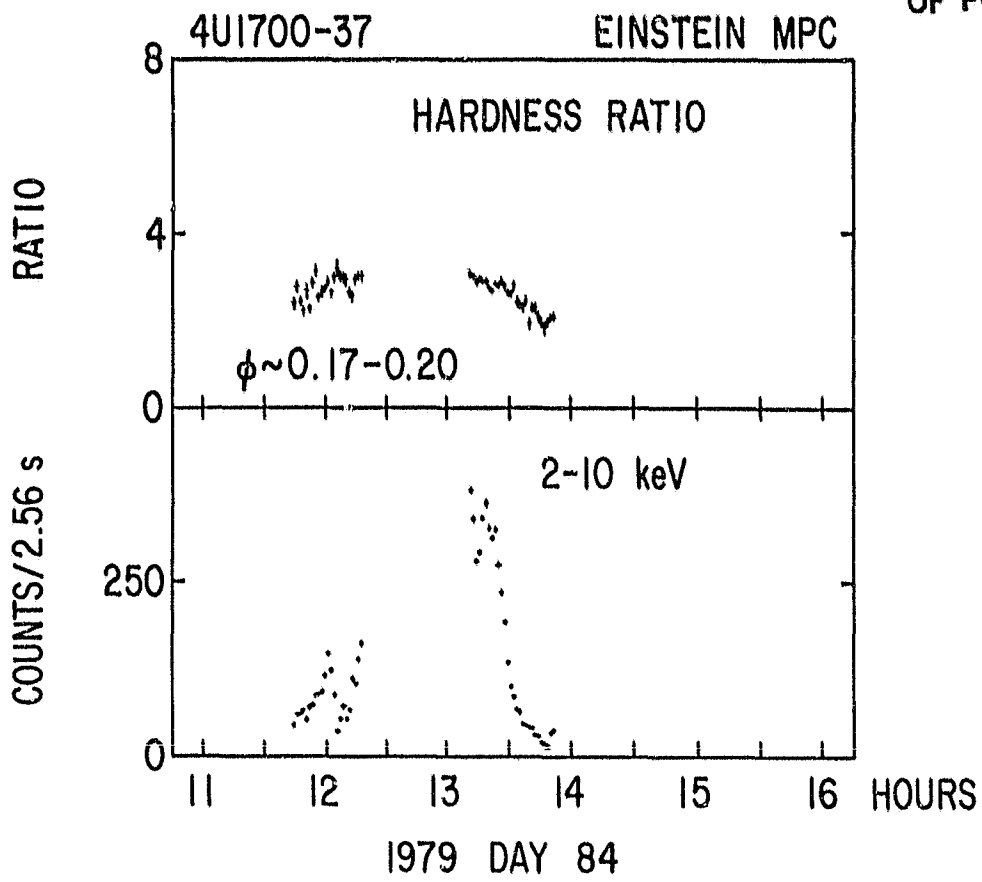
Figure 2 - The 2-10 keV intensity verses time for all the MPC observations of 4U1700-37 in 50 s accumulation intervals. Also shown in the hardness ratio which is the division of the 5-10 keV over the 2-5 keV energy band.

Figure 3 - The hardness ratios and count rates given in Figure 2 plotted against each other. Typical one sigma errors are shown.

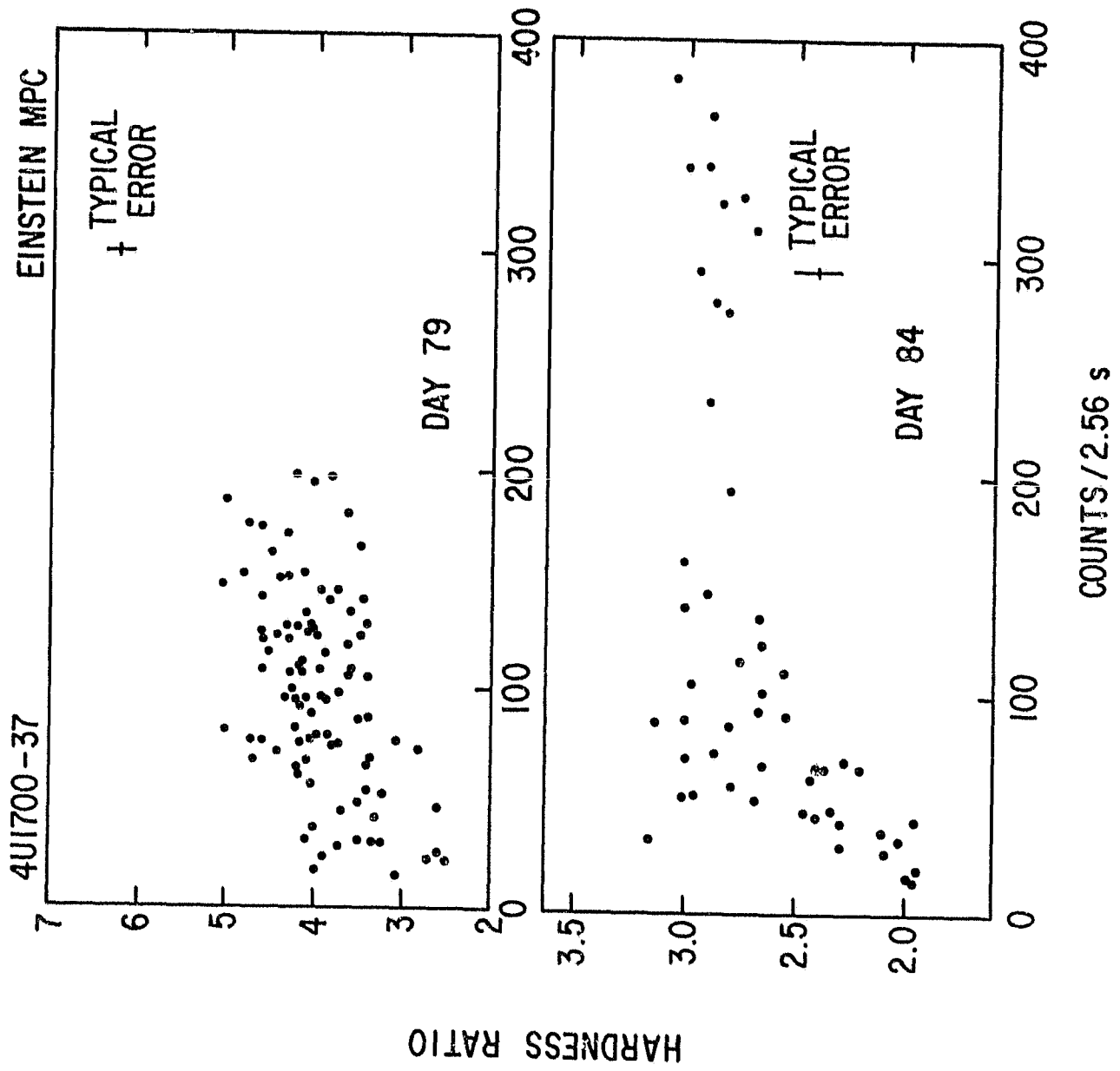
Figure 4 - The PHA spectra from each of the two SSS observations. The flare and non-flare data have been combined. The best fit models given in Table 2 are shown as solid lines. The deviations at energies < 2 keV are caused by uncertainties in the background subtraction.

ORIGINAL PAGE IS
OF POOR QUALITY

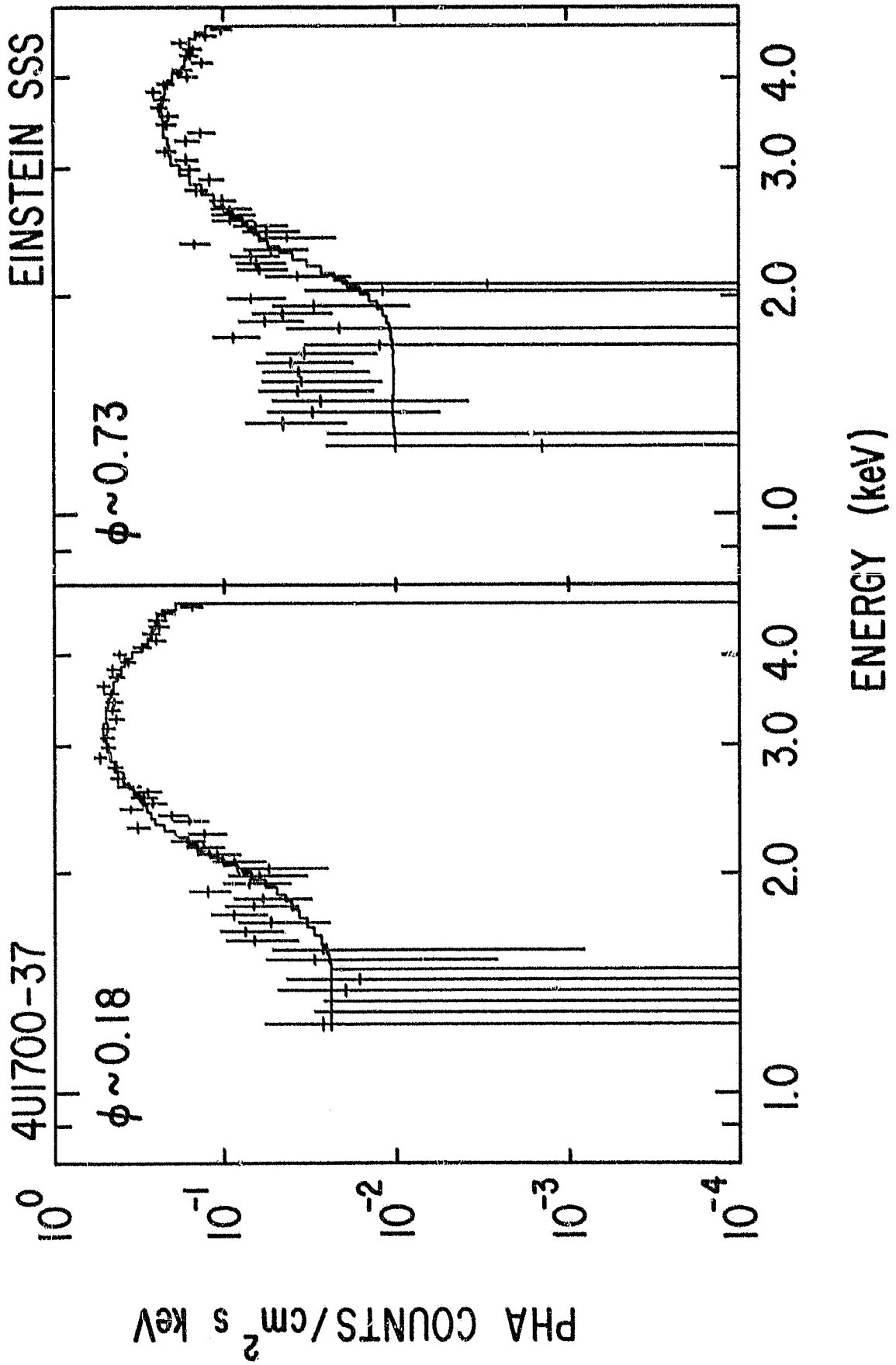




ORIGINAL PAGE IS
OF POOR QUALITY



ORIGINAL PAGE IS
OF POOR QUALITY



AUTHORS' ADDRESSES

J.H. SWANK, N.E. WHITE, Code 661, Laboratory for High Energy Astrophysics,
NASA/Goddard Space Flight Center, Greenbelt, Maryland 20771

T.R. KALLMAN, Center for Space Research and Dept. of Physics, Massachusetts
Institute of Technology, Cambridge, MA 02139

N.E. WHITE, ESTEC, Postbus 299, 2200 A.G. Noordwijk Zh, THE NETHERLANDS